DOI: 10.1002/ejic.200701109

Equilibrium and Kinetic Properties of Cu^{II} Cyclophane Complexes: The Effect of Changes in the Macrocyclic Cavity Caused by Changes in the Substitution at the Aromatic Ring

Begoña Verdejo,[a] Manuel García Basallote,*[b] Armando Ferrer,[b] María Angeles Mañez,[b] Juan Carlos Hernández,[b] Martin Chadim,[c] Jana Hodačová,*[c] José Miguel Llinares,[d] Conxa Soriano,[d] and Enrique García-España*[a]

Dedicated to Professor Ramón Mestre on the occasion of his retirement

Keywords: Cyclophanes / Copper(II) complexes / Protonation constants / Kinetics / Macrocyclic ligands

The *o*-B232, *m*-B232 and *p*-B232 cyclophanes result from attaching the terminal amine groups of 1,4,8,11-tetraazaundecane (232) to the benzylic carbons of the corresponding *o*-, *m*- or *p*-xylanes. The cavity size of these cyclophanes changes moderately as a consequence of the substitution at the aromatic ring. The effects caused by these changes on the equilibrium constants for protonation and Cu^{II} complex formation of the cyclophanes are analyzed and compared with those of the noncyclic 232 polyamine. All three cyclophanes form mononuclear complexes, but only *o*-B232 is able to coordinate to Cu^{II} through the four amine groups simultaneously, whereas *m*-B232 and *p*-B232 can only use three nitrogen donors. The larger cavity and higher flexibility of the latter two cyclophanes allow them to form stable dinuclear Cu^{II} complexes. The kinetics of the acid-promoted dissociation of Cu^{II} from its mono- and dinuclear complexes has also been studied and the results indicate the existence of large differences in the kinetic properties for the complexes with these three closely related ligands. Whereas the mononuclear *m*-B232 and *p*-B232 complexes decompose with very similar kinetic behaviour to that of the $Cu(232)^{2+}$ complex, the lability of the Cu–N bonds is largely reduced in the $Cu(o\text{-}B232)^{2+}$ complex, and this leads to slower decomposition and even to a different rate law for this complex. The dinuclear complexes are not formed with *o*-B232, and very different decomposition kinetics is observed for the complexes formed by *m*-B232 and *p*-B232. In the case of *m*-B232, the two metal ions are situated very close to each other, which causes a rapid release of one of them upon reaction with acid. In contrast, the larger size of *p*-B232 allows it to accommodate two metal ions without important electrostatic or steric interactions so that they are released with statistically controlled kinetics.

Introduction

Polyamine ligands constitute one of the most commonly used families of receptors in coordination chemistry[1] because of their capability to coordinate metal ions and anionic species as a function of the protonation state of the amine groups.[2] These receptors form very stable complexes with 3d metal ions, their stability usually increasing with the number of donor groups because of the chelate effect.[3] For the case of Cu^{II}, open-chain tetraamine ligands such as 1,4,7,10-tetraazadecane (222) and 1,4,8,11-tetraazaundecane (232) form very stable complexes in which the four amine donor groups are arranged in a square-planar disposition around the metal ion.[4] The 232 complexes are more stable than the 222 complexes because of both the higher basicity of the ligand and its capability to form one six-membered chelate ring that reduces the steric constraints associated with tetradentate coordination at the corners of a square.[5,6] In fact, the crystal structure of $[Cu(232)](ClO_4)_2$ shows a square-planar coordination mode for the tetraamine,[7] whereas for the related 222 complex the exclusive formation of five-membered chelate rings forces the metal ion to be situated out of the plane defined by

[a] Departament de Química Inorgànica, Institut de Ciència Molecular (ICMOL),Universitat de València, Edificio de Institutos de Paterna,
Apartado de Correos 22085, 46071 Valencia, Spain
Fax: +34-96-3543274
E-mail: enrique.garcia-es@uv.es
[b] Departamento de Ciencia de los Materiales e Ingenieria Metalúrigica, Facultad de Ciencia, Universidad de Cádiz,
Apdo. 40, Puerto Real, 11510 Cádiz, Spain
E-mail: manuel.basallote@uca.es
[c] Institute of Organic Chemistry and Biochemistry, Academy of Sciences of the Czech Republic,
Flemingovo nam. 2, 16610 Prague 6, Czech Republic
[d] Departament de Química Orgànica, Institut de Ciència Molecular (ICMOL), Universitat de València, Edificio de Institutos de Paterna,
Apartado de Correos 22085, 46071 Valencia, Spain
Supporting information for this article is available on the WWW under http://www.eurjic.org or from the author.

the four nitrogen donors.[8] These differences between very closely related ligands can be useful for medical applications such as the investigation of chelating alternatives for D-penicilamine in the treatment of Wilson's disease, in which large amounts of Cu^{II} are accumulated in the organism.[9,10] In this way, it has been shown that the 232 polyamine leads to higher copper excretion rates than the 222 polyamine or D-penicilamine.[11] Another potential important medical application of this kind of ligand is the development of compounds useful for radiopharmaceutical applications with copper-64, as it has been suggested that cyclic polyamines with a *cyclam* backbone are optimal for these purposes.[12]

The formation of macrocyclic ligands composed of these polyamines and an aromatic spacer (cyclophanes) results in increases in the rigidity and preorganization of the organic molecule, and this has been exploited in recent decades to develop a rich and interesting chemistry[13] that includes the formation of tertiary species suitable for recognition or catalytic purposes.[14] From the point of view of the present work, it is interesting to note that these kinds of complexes can undergo reorganization movements associated with the protonation of the uncoordinated nitrogen atoms, which can be observed by studying the kinetics of the acid-promoted decomposition of the different species of complexes.[15] These reorganization processes resemble some molecular movements occurring in nature that are powered by gradients in the proton concentration such as the rotation of the γ protein in the F_0/F_1 ATP-synthase and the flagellar rotation in bacteria.[16]

Another interesting case is that in which the aromatic spacer causes the donor groups in the polyamine chain to behave as two separate subunits that simultaneously coordinate two metal centres, as occurs in the case of the dinuclear 2,5,8,11-tetraaza[12]paracyclophane (*p*-B222) Cu^{II} complex, whose crystal structure reveals the ligand's bidendate character with respect to each one of the metal centres.[17] Although there is a large amount of information regarding dinuclear complexes formed with cyclophanes and related ligands with a large macrocyclic cavity, the information available regarding the relative stability and, especially, the kinetic properties of the mono- and dinuclear complexes formed with cyclophanes derived from open-chain tetraamines such as 232 is relatively scarce.[18] In this sense, the study of the family of cyclophanes shown in Scheme 1 provides an excellent opportunity to analyze in detail the way in which subtle modifications, such as those caused by a change in the substitution at the aromatic spacer, affect these properties. The synthesis of the *m*-B232 and *p*-B232 ligands is described for the first time in this paper, and these have been used to conduct a comparative equilibrium and kinetic study on their copper complexes (Figure 1).

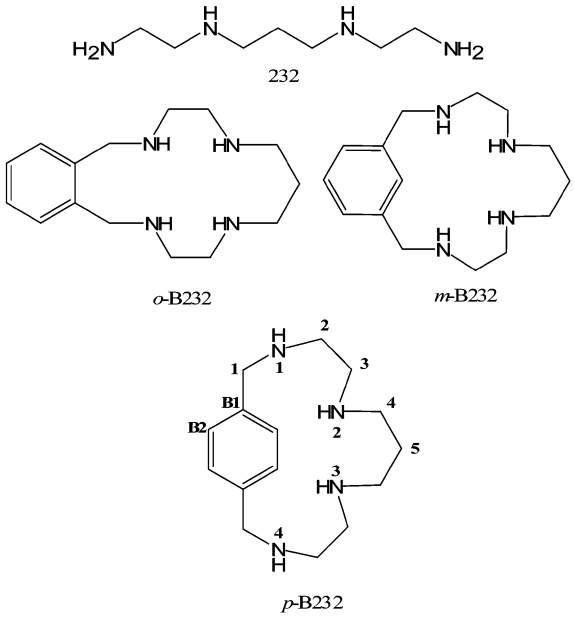

Scheme 1.

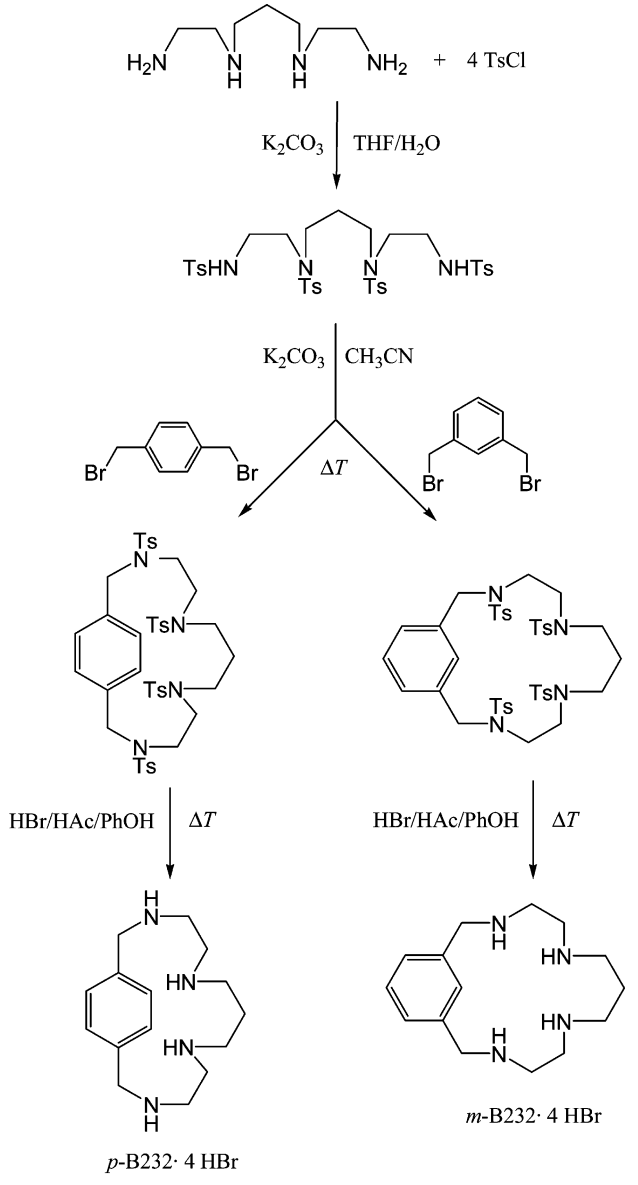

Figure 1. Synthetic pathway for the synthesis of the *m*-B232 and *p*-B232 cyclophanes.

Results and Discussion

Synthesis and Protonation of the Cyclophanes

The *o*-B232 polyamine has been prepared as described previously.[18] The preparation of the new *m*-B232 and *p*-B232 cyclophanes has been carried out using a procedure similar to that previously described for related cyclophane ligands.[15,17] This procedure is depicted in Figure 1 and it consists of three sequential steps involving tosylation of the polyamine, cyclization by reaction with the corresponding dibromoxylene and detosylation to obtain the final products, which were isolated as the tetrahydrobromide adducts. Full details are given in the Experimental section.

The protonation equilibrium constants for the whole series of ligands in Scheme 1 were obtained from the analysis of potentiometric titrations, and their values are included in Table 1. The open-chain 232 ligand shows a significantly higher overall basicity than its cyclic analogues, which can be related to its higher flexibility and higher capability to separate the positive charges created upon protonation. For the case of the cyclophanes, the cyclic nature of the ligands introduces severe constraints on the relative positions of the different amine groups, which results in a decreased basicity. In addition, although the presence of an aromatic spacer forces the separation of the two nitrogen atoms closer to the spacer (Figure 2), it also leads to a lower flexibility. As a consequence, the four successive protonation constants for *m*-B232 and *p*-B232 are smaller than the corresponding constants for 232, the difference increasing with the degree of protonation. However, the behaviour of *o*-B232 is slightly different: the first two protonation processes occur with constants significantly larger than those found for the acyclic 232 ligand. This increased basicity in the early protonation stages can be explained by the formation of intramolecular hydrogen bonds between couples of protonated and unprotonated nitrogen atoms, as revealed by NMR studies at different pH values[21] and by the crystal structure of the $[H_2(o\text{-B232})](picrate)_2 \cdot 1/2(C_3H_6O)$ molecule.[18] As the third and fourth protonation steps involve the breaking of the hydrogen bond network, the values of the corresponding equilibrium constants are smaller than for the other ligands, the fourth one being so small that it cannot be determined from the potentiometric data ($\log K < 2$). These deviations in the values of the protonation constants from a regular trend have been previously observed for cyclam and other ligands.[17–20] The formation of intramolecular hydrogen bonds is strongly favoured by the presence of the *o*-xylyl spacer, but they do not appear to be relevant in the protonation of the related macrocycles containing *m*- and *p*-xylyl spacers.[17]

Table 1. Logarithms of the stepwise protonation constants for 232, *o*-B232, *m*-B232 and *p*-B232 measured in 0.15 mol dm^{-3} $NaClO_4$ at 298.0 ± 0.1 K.

Reaction	232	*o*-B232[d]	*m*-B232	*p*-B232
H + L = HL[a]	10.10(5)[b]	11.01(3)	9.83(8)	9.55(3)
H + HL = H_2L	9.42(3)	9.88(3)	8.60(8)	8.59(3)
H + H_2L = H_3L	7.17(2)	2.20(7)	5.92(1)	5.81(5)
H + H_3L = H_4L	5.76(2)	<2	3.88(1)	4.50(5)
log β[c]	32.45	23.09	28.23	28.45

[a] Charges not included. [b] The numbers in parentheses show the standard deviation in the last significant figure. [c] Cumulative basicity constant for the ligand. [d] Data from ref.[18].

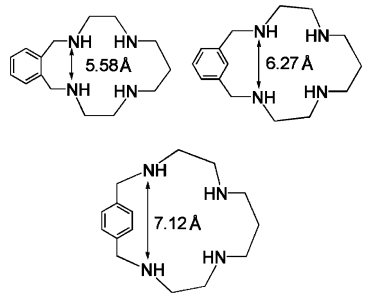

Figure 2. Estimated size of the macrocyclic cavity in the *o*-B232, *m*-B232 and *p*-B232 cyclophanes as calculated with molecular modeling.

The Stability of Cu^{II} Complexes

Table 2 includes the stability constants of the Cu^{II} complexes with the 232, *o*-B232, *m*-B232 and *p*-B232 ligands. These values were derived from the analysis of the potentiometric titrations of solutions containing the metal and the ligand in 1:1 and 2:1 molar ratios at 298.1 K in the presence of 0.15 mol dm^{-3} $NaClO_4$ (for solubility reasons, NaCl was used in the case of *p*-B232).

The data for the 232 and *o*-B232 ligands had been published previously,[5,6,18] and so they will be discussed only briefly for comparative purposes. The equilibrium model for the Cu^{II} complexes of these two ligands is very simple and includes only the formation of CuL^{2+} and $HCuL^{3+}$ species, without any evidence of the formation of dinuclear species. Despite the fact that the crystal structures of the complexes with both ligands are similar with the four amine groups coordinated to the metal centre in the equatorial plane,[7,18] the stability of the CuL^{2+} complex with *o*-B232 is about five orders of magnitude lower than that formed with the acyclic 232 ligand. In contrast, the formation of $HCuL^{3+}$ from CuL^{2+} is more favoured for the cyclic ligand. These observations can be explained by considering the lower basicity of *o*-B232 and the formation of a seven-membered chelate ring in the $Cu(o\text{-B232})^{2+}$ species.

The equilibrium model required for a satisfactory fit of the data for the *m*-B232 and *p*-B232 cyclophanes is more complex, with the formation of additional mononuclear [H_2CuL^{4+}, H_3CuL^{5+} and $CuL(OH)^{+}$] and dinuclear [Cu_2L^{4+}, $Cu_2L(OH)^{3+}$ and $Cu_2L(OH)_2^{2+}$] species. It is important to note that because of the close proximity of the metal centres in the dinuclear complexes, conversion to hydroxo-bridged species is favoured for both cyclophanes as a way to reduce electrostatic repulsion. As expected from the size of the macrocyclic cavity, the stability of the dinuclear species is higher in the case of *p*-B232. The same

Table 2. Logarithms of the stability constants for the formation of Cu^{II} complexes with the 232, *o*-B232, *m*-B232 and *p*-B232 ligands measured in 0.15 mol dm^{-3} $NaClO_4$ at 298.0 ± 0.1 K.

Reaction[a]	232[b]	*o*-B232[c]	*m*-B232	*p*-B232[d]
M + L ⇆ ML	23.30(1)	17.73(3)	13.29(1)	12.71(1)
M + H + L ⇆ MHL	26.38(3)	21.62(5)	20.48(4)	18.80(9)
M + 2 H + L ⇆ MH_2L	–	–	24.11(1)	23.69(1)
M + 3 H + L ⇆ MH_3L	–	–	–	27.83(1)
M + L + H_2O ⇆ ML(OH) + H	–	–	4.15(2)	–
2 M + L ⇆ M_2L	–	–	–	16.81(2)
2 ML + L + H_2O ⇆ $M_2L(OH)$ + H	–	–	9.31(9)	–
2 ML + L + H_2O ⇆ $M_2L(OH)_2$ + H	–	–	3.28(1)	5.96(1)

[a] Charges not included. [b] The numbers in parentheses show the standard deviation in the last significant figure. [c] Data from ref.[18] [d] Measured in 0.15 mol dm^{-3} NaCl: $\log K_{HL/H\cdot L}$ = 9.82(5), $\log K_{H2L/H\cdot HL}$ = 8.57(5), $\log K_{H3L/H\cdot H2L}$ = 5.77(8), $\log K_{H4L/H\cdot H3L}$ = 4.41(8).

model was previously used for the related *p*-B222 ligand, although in that case the shorter length of the polyamine leads to a smaller cavity size and to less stable dinuclear species [$\log\beta$ = 3.44 for the Cu_2(*p*-B222)$(OH)_2^{2+}$ species vs. 5.96 for the corresponding *p*-B232 species]. The symmetrical nature of the *m*-B232 and *p*-B232 ligands makes it reasonable to think that the structure of the dinuclear complexes is similar to that previously reported for [Cu_2(*p*-B222)Cl_4],[17] in which each metal centre is coordinated to two of the amine groups in the cyclophane.

The stability of the mononuclear CuL^{2+} species with the *m*-B232 and *p*-B232 ligands is very similar to and about four orders of magnitude lower than that of the related *o*-B232 complex, which suggests that changing the substitution at the aromatic ring from *ortho* to *meta* or *para* causes a change in the coordination mode of the cyclophanes. However, as the *p*-B232 data were obtained in the presence of Cl^- and the crystal structure of the Cu(*o*-B232)$^{2+}$ complex also reveals the presence of a coordinated chloride, it can be argued that these differences in the equilibrium constants are caused, at least in part, by the change in the nature of the supporting electrolyte. Nevertheless, although precipitation hinders the determination of the complete set of equilibrium constants for the Cu^{II}–*p*-B232 system in 0.15 mol dm^{-3} $NaClO_4$, the analysis of potentiometric data in this medium allows for the determination of the stability of the mononuclear species and the results indicate that $\log K$ for the formation of Cu(*p*-B232)$^{2+}$ is 12.05. This value is quite close to that in Table 2 and shows that changing the nature of the anion in the supporting electrolyte from chloride to perchlorate does not lead to large changes in the stability of the metal complexes; therefore the stability differences found for the three cyclophanes must be mainly associated with changes in the nature of the ligand. Whereas for *o*-B232 all four nitrogen donors are able to coordinate simultaneously to the metal centre, in the case of *m*-B232 and *p*-B232 the substitution at the aromatic ring hinders the simultaneous coordination of the two benzylic nitrogen atoms and the ligand can only use a maximum of three donor groups in the formation of mononuclear complexes (see Figure 3).[22] In agreement with this conclusion, a similar behaviour is observed for the complexes with cyclophanes derived from the related 222 polyamine: $\log K$ for the formation of Cu(*m*-B222)$^{2+}$ is 13.52 whereas this value for the related *o*-B222 species (19.58) is several orders of magnitude higher.[18]

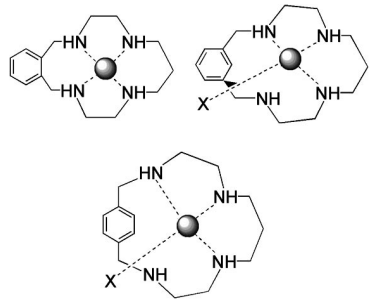

Figure 3. Schematic representation of copper coordination with *m*-B232, *o*-B232 and *p*-B232.

Additional information about the dentate character of the cyclophanes in the CuL^{2+} species can be obtained by comparing the values of its protonation constants with those of the free ligand species with the same charge. Although deriving coordination numbers just from free energy terms can often be misleading, a careful consideration of the protonation constants of the complexes as well as comparison with related systems may be useful in some instances. In this way, it is found that the conversion of CuL^{2+} to $HCuL^{3+}$ ($CuL^{2+} + H^+ \leftrightarrows CuHL^{3+}$; $\log K$ = 7.19 and 6.09 for *m*-B232 and *p*-B232, respectively) occurs with constants higher than those corresponding to the protonation of H_2L^{2+} to give H_3L^{3+} ($\log K$ = 5.92 and 5.81 for *m*-B232 and *p*-B232, respectively), which clearly indicates that the first protonation of the metal complex occurs at a noncoordinated amine group. Moreover, as the $\log K$ values for the formation of the Cu(*m*-B232)$^{2+}$ and Cu(*p*-B232)$^{2+}$ species are close to those found for related polyamines acting as tridentate ligands,[17,23] it is reasonable to conclude that *m*-B232 and *p*-B232 coordinate to the metal centre in CuL^{2+} using the two central and one of the benzylic amine groups, the other benzylic nitrogen remaining uncoordinated.

Kinetics of the Acid-Promoted Decomposition of the Cu^{II} Complexes

As an example, the species distribution curves corresponding to the formation of Cu^{II} complexes in solutions containing Cu^{II} and *m*-B232 in 1:1 and 2:1 molar ratios are included in Figure 4, which shows that solutions with equimolar amounts of metal and cyclophane contain mononuclear species with a protonation degree that changes with pH and that the formation of dinuclear complexes is negligible. In contrast, the dinuclear complexes dominate the distribution curves in neutral and basic solutions containing a 2:1 molar ratio (Cu/L). The distribution curves for the formation of metal complexes with the other ligands are included in the Supporting Information.

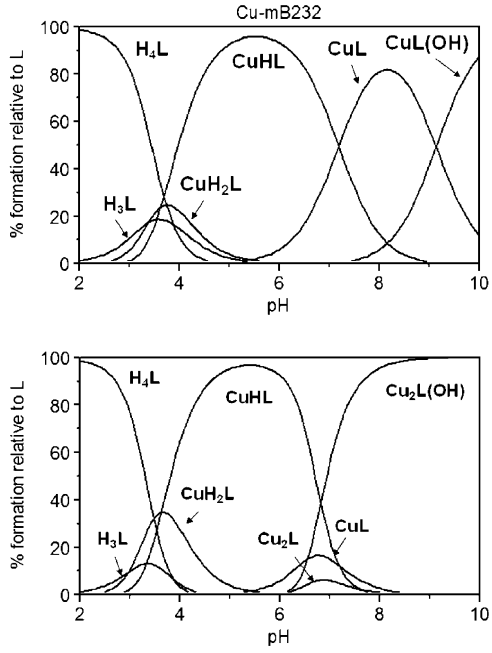

Figure 4. Species distribution curves for the formation of Cu^{II} complexes with the *m*-B232 cyclophane. The curves were obtained using [L] = 1.0×10^{-3} mol dm^{-3} and Cu^{II} in 1:1 (top) or 2:1 (bottom) molar ratios.

Inspection of the species distribution curves for the different Cu^{II}–L systems indicates that the degree of complexation is negligible in strongly acidic solutions; therefore, the addition of an excess of acid to a solution of the complexes will result in complex decomposition with formation of $Cu^{2+}_{(aq)}$ and the corresponding protonated form of the ligand [Equation (1)]. For other Cu^{II} polyamine systems, the kinetics of this process has been found to occur over time scales that span from sub-millisecond to days (or more) in duration, with this being dependent on the lability of the metal–ligand bonds. Although most of the literature kinetic studies on complex decomposition have been carried out by adding the acid excess to a solution prepared from a solid sample of the complex, we have previously demonstrated that the kinetics of complex decomposition can be significantly different for closely related species such as those resulting from the protonation or hydroxylation of the CuL^{2+} complexes.[15,23] For this reason, it is necessary to control the pH of the starting complex solution in these kinetic studies by selecting pH values at which the distribution curves indicate the existence of a single major species. The application of this criterion to the ligands studied in the present work indicates that the only species whose decomposition kinetics can be measured without interference from significant amounts of other species in equilibrium are $Cu(232)^{2+}$, $Cu(o\text{-B232})^{2+}$, $HCu(m\text{-B232})^{3+}$, $Cu(m\text{-B232})^{2+}$, $Cu(m\text{-B232})OH^{+}$, $Cu_2(m\text{-B232})(OH)_2^{2+}$ and $Cu_2(p\text{-B232})(OH)_2^{2+}$. A kinetic study on the decomposition of these species according to Equation (1) was carried out to analyze the effects caused by changes in the size of the macrocyclic cavity and its results are summarized in Table 3.

$$H_yCu_xL^{2x+} + H^+_{exc} \rightarrow x\,Cu^{2+} + H_nL^{n+} \quad (1)$$

Table 3. Summary of the kinetic data for the decomposition of the Cu^{II} complexes with the 232, *o*-B232, *m*-B232 and *p*-B232 ligands measured in 0.15 mol dm^{-3} $NaClO_4$ at 298.0 ± 0.1 K.

Species	Rate law[a]	Kinetic parameters[b]
$Cu(232)^{2+}$ [c]	$bc[H^+]/(1 + c[H^+])$	b = 0.35(2) s^{-1} c = 50(6) mol^{-1} dm^3
$Cu(o\text{-B232})^{2+}$ [d]	$d[H^+]^2 + e$	$d = 1.9(2) \times 10^{-4}$ mol^{-2} dm^6 s^{-1} $e = 1.1(3) \times 10^{-5}$ s^{-1}
$HCu(m\text{-B232})^{3+}$	$a + bc[H^+]$ [e]	a = 0.5(2) s^{-1} bc = 118(5) mol^{-1} dm^3 s^{-1}
	$bc[H^+]$ [f]	bc = 2.55(7) mol^{-1} dm^3 s^{-1}
$Cu(m\text{-B232})^{2+}$	[g]	
$Cu(m\text{-B232})(OH)^{+}$	[g]	
$Cu_2(m\text{-B232})(OH)_2^{2+}$	[h]	
$Cu_2(p\text{-B232})(OH)_2^{2+}$ [i]	$a + bc[H^+]$	a = 0.59(7) s^{-1} bc = 8.6(4) mol^{-1} dm^3 s^{-1}

[a] See explanation in the text. [b] The numbers in parentheses show the standard deviation in the last significant figure. [c] Similar results are obtained when the supporting electrolyte is changed from $NaClO_4$ to NaCl or KNO_3. [d] Data obtained in 1.0 mol dm^{-3} $NaClO_4$. [e] First resolved kinetic step. [f] Second resolved kinetic step. [g] The decomposition of these species occurs with the same kinetics as for $HCu(m\text{-B232})^{3+}$. [h] The decomposition of this species starts with a very fast step (<1.7 ms) that leads to a mononuclear species, which decomposes more slowly with the same kinetics as for $HCu(m\text{-B232})^{3+}$. [i] Data obtained in 0.15 mol dm^{-3} NaCl.

Ligands 232 and *o*-B232 only form mononuclear Cu^{II} complexes, the CuL^{2+} species showing in both cases a single absorbance band with maxima centred at similar wavelengths [530 nm for $Cu(232)^{2+}$ and 540 nm for $Cu(o\text{-B232})^{2+}$]; this suggests that the coordination environment around the metal centre is the same, surely with all four nitrogen donors of the ligand coordinated, as revealed by the crystal structure of the complexes.[7,18] Despite the similarity of the structure and absorption band in both complexes, the decomposition kinetics of $Cu(232)^{2+}$ and $Cu(o\text{-B232})^{2+}$ is very different. For the complex with the noncyclic 232 polyamine, the reaction occurs in the stopped-flow time scale and leads to complete decomposition of the complex, as revealed by the complete disappearance of the absorption band typical of the complex (Figure 5). The process occurs in a single kinetic step with observed rate con-

stants that show saturation behaviour with respect to the acid concentration [Figure 6 and Equation (2)]. The rate constants were found to be independent of the nature of the salt used as supporting electrolyte and, actually, the data in Figure 6 were obtained by averaging the results obtained in the presence of $NaClO_4$, NaCl or KNO_3 (0.15 mol dm^{-3}). The values obtained from the fit of the experimental data to Equation (2) are $b = (0.35 \pm 0.02)$ s^{-1} and $c = (50 \pm 6)$ mol^{-1} dm^3, a being negligible. These results are in good agreement with literature data,[24] although there are small differences that can be related to the different concentrations of supporting electrolyte used, as ionic strength effects are expected to be important in this kind of reaction between charged species.

$$k_{obs} = \frac{a + bc[H^+]}{1 + c[H^+]} \quad (2)$$

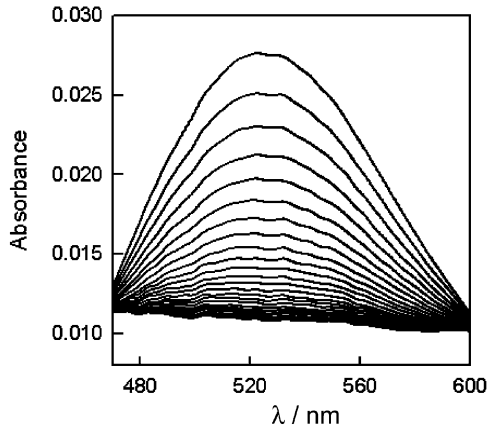

Figure 5. Typical spectral changes observed during the acid-promoted decomposition of the Cu(232)$^{2+}$ complex. Plotted spectra were recorded at 0.825 s intervals and show the complete disappearance of the Cu(232)$^{2+}$ absorbance centred at ca. 530 nm.

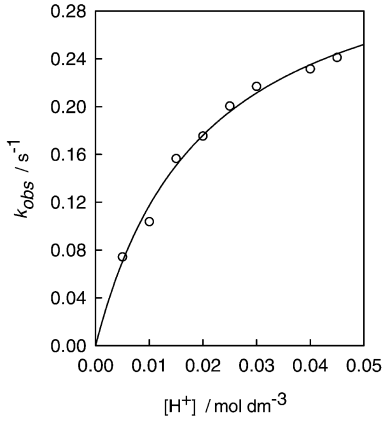

Figure 6. Plot of the acid concentration dependence of the observed rate constant for the acid-promoted decomposition of the Cu^{II} complexes with the 232 ligand.

With regard to the intimate mechanism of decomposition of Cu(232)$^{2+}$, the experimental rate law in Equation (2) can be interpreted in terms of the classical mechanism proposed by Margerum and other workers,[15,24,25] which assumes that dissociation of the Cu–N bond in the rate-determining step occurs with the formation of an activated intermediate, (CuL^{2+})*, with an increased Cu–N distance under steady-state conditions [Equation (3)]. However, in this intermediate there is no complete breaking of the bond; this is only completed upon acid (k_H) or solvent (k_{H_2O}) attack [Equations (4) and (5)]. As this intermediate is formed under steady-state conditions, its concentration remains too low during the whole decomposition process and so it is not detectable in the kinetic traces, which simply show absorbance changes with time according to a single exponential. When the rate of decomposition through solvent attack is much slower than that corresponding to acid attack, the rate law has the same form as Equation (2), with the a term being negligible, and $b = k_1$ and $c = k_H/k_{-1}$, where the constants k_1 and k_{-1} represent the rate constants for the reversible formation of the activated (CuL^{2+})* intermediate from the starting complex. According to this mechanism, the value of $k_1 = (0.35 \pm 0.02)$ s^{-1} provides information about the lability of the Cu–N bond.

$$CuL^{2+} \leftrightarrows (CuL^{2+})^*;\ k_1,\ k_{-1} \quad (3)$$

$$(CuL^{2+})^* + H^+ \rightarrow Cu^{2+}{}_{(aq)} + H_xL^{x+};\ k_H \quad (4)$$

$$(CuL^{2+})^* + H_2O \rightarrow Cu^{2+}{}_{(aq)} + H_xL^{x+};\ k_{H_2O} \quad (5)$$

Although decomposition of the Cu(o-B232)$^{2+}$ complex also occurs in a single measurable kinetic step, the process is several orders of magnitude slower and it could only be made to occur to a significant extent by increasing the acid concentration by an order of magnitude, which also required an increase in the concentration of the supporting electrolyte up to 1.0 mol dm^{-3} $NaClO_4$. Even under those conditions, complete decomposition of the complex was not achieved in all cases and the process occurs under equilibrium conditions at [H$^+$] as high as 0.1–0.2 mol dm^{-3}. The dependence of the observed rate constant on the acid concentration is also different, the plot of k_{obs} vs. [H$^+$] showing the existence of a nonzero intercept and a second-order dependence on the acid concentration (Figure 7). These data could be reasonably well fit to Equation (6), with values of $e = (1.1 \pm 0.3) \times 10^{-5}$ s^{-1} and $d = (1.9 \pm 0.2) \times 10^{-4}$ mol^{-2} dm^6 s^{-1}. Although a second-order dependence with respect to the acid concentration has been previously reported for the decomposition of other complexes,[26] to the best of our knowledge there is only a single recent report in which this dependence coexists with a nonzero intercept in the rate law for the decomposition of Cu^{II} polyamine complexes.[27]

Interpreting the rate law in Equation (6) in terms of the Margerum's mechanism requires that the rate-determining step be associated with the breaking of the second Cu–N bond rather than the dissociation of the first one. Given that the process occurs under reversible equilibrium conditions, the experimental data can be interpreted with the mechanism shown in Equations (7), (8) and (9), which indicates that acid attack on the activated intermediate to break the first bond does not result in complex decomposition but

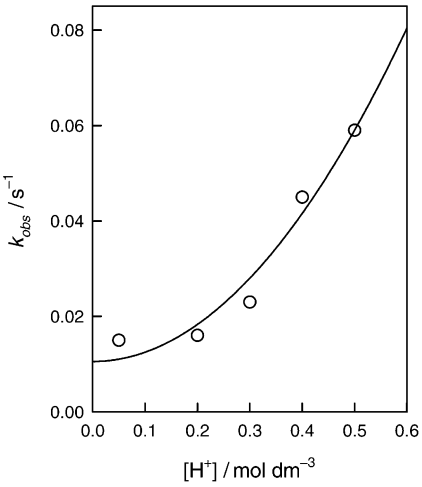

Figure 7. Plot of the acid concentration dependence of the observed rate constant for the acid-promoted decomposition of the Cu^{II} complexes with the *o*-B232 ligand.

leads to the formation of a new I* intermediate that requires attack by a second proton. If the processes in Equations (7) and (8) occur under conditions of reversible equilibria largely displaced to the left-hand side, the rate law for this mechanism has the same form as in Equation (6) with the equivalencies $d = K_1K_{H1}k_2$ and $e = k_{-2}$. As the nonzero intercept can be related to the contribution of the reverse process to the rate of reaction, there is no need to include a k_{H_2O} term for solvent attack, as was the case for the other complex with the same kinetics of decomposition.[27] Regardless, some contribution to the *e* term from parallel water attack cannot be ruled out in the case of Cu(*o*-B232)$^{2+}$ on the basis of the current experimental data.

$$k_{obs} = e + d[H^+]^2 \quad (6)$$

$$CuL^{2+} \leftrightarrows (CuL^{2+})^*;\ k_1,\ k_{-1},\ K_1 \quad (7)$$

$$(CuL^{2+})^* + H^+ \leftrightarrows I^*;\ k_{H1},\ k_{-H1},\ K_{H1} \quad (8)$$

$$I^* + H^+ \leftrightarrows Cu^{2+} + H_xL^{x+};\ k_2,\ k_{-2};\ K_2 \quad (9)$$

The acquisition of very different results for the decomposition of the closely related Cu(232)$^{2+}$ and Cu(*o*-B232)$^{2+}$ complexes deserves some additional commentary. Although it can be intuitively thought that the kinetics of complex decomposition must be correlated with the stability of the decomposing complex, the present data clearly illustrate that complex stability is not the major factor in determining the rate of complex decomposition. Actually, Cu(*o*-B232)$^{2+}$ decomposes with rate constants four to five orders of magnitude slower than Cu(232)$^{2+}$, despite the higher stability of the latter species by more than five orders of magnitude. It has been proposed that the rate of demetallation of metal polyamine complexes can be correlated with the deviations of the coordination environment around the metal centre with respect to ideal geometries, the more distorted complexes decomposing faster.[26,28] However, although the size of the cavity in *o*-B232 appears to exactly match the size of the Cu^{II} ion,[18] the more flexible noncyclic 232 ligand is also able to arrange itself in a similar way around the metal ion without introducing important steric constraints[7] and, actually, Cu(232)$^{2+}$ decomposes more slowly than complexes with other tetraamines that form more distorted complexes.[24] To understand the very different decomposition kinetics of the Cu^{II} complexes with 232 and *o*-B232, it must be remembered that the reaction kinetics is not only determined by the starting reagents, but also depend on the chemical transformations occurring along the reaction coordinate. As the decomposition process starts with the elongation of the Cu–N bond (k_1 step), complexation with a ligand such as *o*-B232, which not only readily accommodates a metal ion, but also introduces serious constraints on the lengthening of the metal–ligand bonds, will lead to a significant decrease in the rate of decomposition with respect to similar complexes with ligands that are more flexible and able to reorganize more easily upon an increase in the Cu–N distance. The present results would thus indicate that the Cu(*o*-B232)$^{2+}$ structure hinders elongation of the Cu–N bond and makes the distortion achieved in the k_1 step too small to lead to complete complex decomposition upon attack by a single H^+, so that a second proton attack is required. In contrast, the flexibility of the noncyclic 232 ligand allows for the formation of an activated intermediate, $(CuL^{2+})^*$, with a larger increase of the metal–ligand distance, which results in faster decomposition upon proton attack.

As a consequence of their higher cavity size, the *m*-B232 and *p*-B232 cyclophane ligands are able to simultaneously coordinate two metal ions to thus yield binuclear species. For the case of *m*-B232, Cu_2(*m*-B232)$(OH)_2^{2+}$ is the major species in basic solutions containing Cu^{II} and *m*-B232 in a 2:1 molar ratio. The corresponding $Cu_2L(OH)^{3+}$ complex only exists as a minor species, and Cu_2L^{4+} cannot be detected in the potentiometric studies This suggests that although the size of this cyclophane allows for the simultaneous coordination of two metal ions, these are forced to be too close to each other and a significant stability is only achieved when two OH^- bridges reduce the electrostatic repulsion between the dipositive centres. In agreement with these considerations, the kinetic studies on the decomposition of Cu_2(*m*-B232)$(OH)_2^{2+}$ indicate that upon addition of an excess of acid there is a rapid release of one of the metal ions within the mixing time of the stopped-flow instrument (ca. 1.7 ms), and that this process is followed by the slower decomposition of the resulting mononuclear complex [Equations (10) and (11)]. The latter process occurs with the same kinetics that is observed when the decomposition is studied using starting solutions containing the mononuclear HCu(*m*-B232)$^{3+}$, Cu(*m*-B232)$^{2+}$ or Cu(*m*-B232)$(OH)^+$ complexes, which indicates that the protonation processes associated with the interconversion of these species are very fast and that the decomposition of the more protonated HCu(m-B232)$^{3+}$ species is the kinetic process being monitored in all cases. This observation is also in agreement with the stability results, which showed that not all of the amino groups in *m*-B232 coordinate simultaneously to a single

metal ion, so that one of them remains uncoordinated and behaves as a free amine, which results in very rapid protonation. The disappearance of the absorption band at 580 nm associated with the release of the metal ion from HCu(*m*-B232)$^{3+}$ occurs with biphasic kinetics, the rate constants for both resolved steps showing a linear dependence with respect to the acid concentration (Figure 8). These results can be fit to Equation (12) with $a = (0.5 \pm 0.2)\ s^{-1}$ and $bc = (118 \pm 5)\ mol^{-1}\,dm^3\,s^{-1}$ for the first step, and with a negligible value for a and $bc = (2.55 \pm 0.07)\ mol^{-1}\,dm^3\,s^{-1}$ for the second step. This rate law can also be interpreted on the basis of the classical mechanism of decomposition discussed above, although the existence of a nonzero intercept for the first step indicates that in this case there is a significant contribution of the solvent attack (k_{H_2O}) to the rate of complex decomposition. The quotient bc/a corresponds to the k_H/k_{H_2O} ratio and provides information about the relative rates of decomposition through the parallel attacks by H^+ and H_2O.[23] Unfortunately, the absence of curvature in the plots in Figure 6 precludes the estimation of the lability of the Cu–N bonds through the resolution of values for *b*. In any case, the values of the product *bc* for both steps is less than an order of magnitude different from the value for the complex with the noncyclic 232 ligand ($17.5\ mol^{-1}\,dm^3\,s^{-1}$), which suggests that coordination of only three of the four amine groups in the *m*-B232 complex leads to a kinetic behaviour that resembles that of the acyclic ligands, a situation very different from that found for *o*-B232.

$$Cu_2(m\text{-B232})(OH)_2^{2+} + H^+_{exc} \rightarrow Cu^{2+} + HCu(m\text{-B232})^{3+} \quad (10)$$

$$HCu(m\text{-B232})^{3+} + H^+_{exc} \rightarrow Cu^{2+} + H_4(m\text{-B232})^{4+} \quad (11)$$

$$k_{obs} = a + bc[H^+] \quad (12)$$

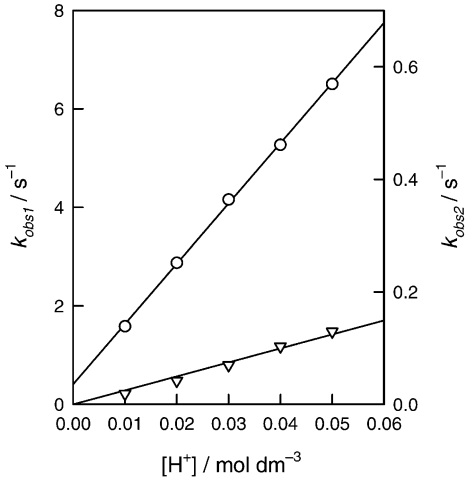

Figure 8. Plot of the acid concentration dependence of the observed rate constants for the acid-promoted decomposition of the mononuclear Cu^{II} complexes with the *m*-B232 ligand. The circles and the triangles correspond to the k_{1obs} and k_{2obs}, respectively.

For the case of *p*-B232, the distribution curves for solutions with 1:1 molar ratios show that there are no pH values at which any of the mononuclear species exist without significant amounts of other species in equilibrium; therefore, a separate kinetic study of the decomposition of the different species is not possible. In any case, experiments were carried out that monitored the kinetics of decomposition of solutions containing a mixture of mononuclear species, which allowed the observation of the disappearance of a band at 580 nm in a single kinetic step. The values of k_{obs} for this process show a dependence with respect to the acid concentration that can also be fit to Equation (12) with $bc = 48 \pm 2\ mol^{-1}\,dm^3\,s^{-1}$ and a negligible value of a. These values indicate that the decomposition kinetics of the mononuclear *p*-B232 complexes does not appear to be very different from those observed for the 232 complex, which is in agreement with an increase in the flexibility of the cyclophane complexes as the cavity size increases.

For *p*-B232, the cyclophane with the largest cavity size of those studied in the present work, the equilibrium behaviour also shows the formation of a stable $Cu_2L(OH)_2^{2+}$ complex as the major species in basic solutions containing Cu^{II} and L in a 2:1 molar ratio. This species shows an electronic absorption spectrum with an absorption band centred at 660 nm that disappears slowly upon addition of excess acid. The process occurs in a single kinetic step with rate constants whose dependence on the acid concentration can also be fit to Equation (12) with $a = 0.59 \pm 0.07\ s^{-1}$ and $bc = 8.6 \pm 0.4\ mol^{-1}\,dm^3\,s^{-1}$. It is important to note that the initial spectrum recorded in the stopped-flow experiments for the decomposition of $Cu_2(p\text{-B232})(OH)_2^{2+}$ coincides with that recorded for the dinuclear complex (band at 660 nm), so that the process whose kinetics is being monitored is that represented by Equation (13). In contrast, for the related dinuclear *m*-B232 complex, the initial spectrum in the kinetic experiments shows the band of the mononuclear species, which thus shows the rapid release of one metal ion from the dinuclear species [Equations (10) and (11)].

$$Cu_2(p\text{-B232})(OH)_2^{2+} + H^+_{exc} \rightarrow 2Cu^{2+} + H_4(p\text{-B232})^{4+} \quad (13)$$

The observation of a single kinetic step for the release of two metal ions from a binuclear complex has been previously observed for other systems and has been interpreted in terms of the statistically controlled dissociation kinetics of both metal ions.[29] This indicates that the size of the *p*-B232 cyclophane allows for the simultaneous coordination of two metal ions without significant electronic or steric interaction between them, so that they behave as independent reacting centres and dissociate with rate constants differing only in the statistical 2:1 ratio, in the same way as dinuclear complexes with macrocycles of larger size.

Conclusions

As a whole, the stability and kinetic data in this paper indicate that subtle changes in the size of the macrocyclic

cavity of cyclophanes derived from the 232 open-chain tetraamine lead to gradual but relevant changes in the properties of their Cu^{II} complexes. For the smaller member of the series (*o*-B232), a single metal ion is tightly coordinated to the four amine groups to yield a very stable complex that decomposes very slowly upon acid attack. When the substitution at the aromatic ring changes to *meta* or *para*, one of the benzylic amine groups cannot coordinate to the metal ion and the stability of the mononuclear complexes decreases by several orders of magnitude. In contrast, tridentate coordination allows for higher flexibility and the complexes decompose faster, with kinetic behaviour quite close to that of the open-chain 232 ligand. The higher members of the series (*m*-B232 and *p*-B232) are also able to form dinuclear species whose stabilities increase with the size of the macrocyclic cavity. Whereas the size of the *p*-B232 complex is large enough to allow for the metal centres to behave independently with respect to dissociation and thus decompose with statistically controlled kinetics, for the case of *m*-B232 the metal ions are situated closer to each other and one of them dissociates very rapidly upon reaction with acid. These results demonstrate that the kinetics of demetallation of macrocyclic Cu^{II} complexes can be finely tuned by introducing minor modifications in the ligand structure, which can be exploited, for example, when designing copper-64 radiopharmaceuticals.

Experimental Section

***N*,*N*′,*N*″,*N*‴-Tetratosylbis(2-aminoethyl)propylenediamine (232·4Ts):** Bis(2-aminoethyl)propylenediamine (1.5 g, 9.4 mmol) dissolved in THF (400 mL) was mixed with K_2CO_3 (5.3 g, 38.1 mmol) dissolved in water (100 mL). Tosyl chloride (7.4 g, 38.8 mmol) dissolved in THF (100 mL) was then added dropwise to the mixture and this was stirred for a further 24 h. Then the organic phase was separated and vacuum evaporated to dryness. The residue was heated at reflux in EtOH, and the resulting solid was filtered and extensively washed with EtOH; yield 5.5 g, 75%; m.p. 60–62 °C. ^{1}H NMR ($CDCl_3$, 300 MHz): δ = 7.75 (d, J = 8 Hz, 4 H), 7.63 (d, J = 8 Hz, 4 H), 7.29 (t, J = 7 Hz, 8 H), 5.75 (t, J = 6 Hz, 2 H), 3.17 (s, 6 H), 3.11 (t, J = 7 Hz, 6 H), 2.42 (s, 6 H), 2.40 (s, 6 H), 2.00–1.93 (m, 2 H) ppm. ^{13}C NMR ($CDCl_3$, 75.43 MHz), δ = 143.8, 143.4, 136.8, 134.7, 129.9, 129.7, 127.3, 127.0, 50.3, 48.4, 43.4, 28.5, 21.5 ppm. MS (FAB): m/z = 777 $[M + H]^+$.

***N*,*N*′,*N*″,*N*‴-Tetratosyl-2,5,9,12-tetraaza[13]metacyclophane (*m*-B232·4Ts):** 232·4Ts (3.7 g, 4.8 mmol) and K_2CO_3 (6.7 g, 48.2 mmol) in dry CH_3CN (50 mL) was placed in a round-bottomed flask. A solution of 1,3-bis(bromomethyl)benzene (1.3 g, 4.8 mmol) in dry CH_3CN (30 mL) was then slowly added to this, and the mixture was heated at reflux under a nitrogen atmosphere for 24 h and then filtered. The solution was vacuum evaporated to dryness, and the oily product was taken up into EtOH and heated at reflux to obtain a white solid (3.2 g, 76%). M.p. 119–121 °C. ^{1}H NMR ($CDCl_3$, 300 MHz): δ = 7.75 (d, J = 8 Hz, 4 H), 7.64 (d, J = 8 Hz, 4 H), 7.32 (d, J = 8 Hz, 4 H), 7.27 (d, J = 8 Hz, 4 H), 4.06 (s, 4 H), 2.96–2.93 (m, 4 H), 2.83–2.71 (m, 8 H), 2.40 (s, 6 H), 2.36 (s, 6 H), 2.40–2.30 (m, 2 H) ppm. ^{13}C NMR ($CDCl_3$, 75.43 MHz): δ = 144.4, 144.2, 137.2, 134.2, 133.9, 130.4, 130.3, 129.6, 129.5, 128.2, 127.2, 55.1, 50.0, 49.3, 49.2, 22.0, 21.9 ppm. MS (FAB): m/z = 879 $[M + H]^+$.

***N*,*N*′,*N*″,*N*‴-Tetratosyl-2,5,9,12-tetraaza[13]paracyclophane (*p*-B232·4Ts):** This compound was obtained by following the same procedure as that for the synthesis of *m*-B232·4Ts but with 1,4-bis(bromomethyl)benzene as a spacer; yield 3.7 g, 87%; m.p. 176–178 °C. ^{1}H NMR ($CDCl_3$, 300 MHz): δ = 7.72 (d, J = 8 Hz, 4 H), 7.61 (d, J = 8 Hz, 4 H), 7.31 (d, J = 8 Hz, 4 H), 7.26 (d, J = 8 Hz, 4 H), 4.07 (s, 4 H), 3.01–2.95 (m, 4 H), 2.80–2.75 (m, 4 H), 2.70 (t, J = 6 Hz, 4 H), 2.40 (s, 6 H), 2.37 (s, 6 H), 2.40–2.30 (m, 2 H) ppm. ^{13}C NMR ($CDCl_3$, 75.43 MHz), δ = 144.3, 144.0, 136.6, 135.0, 134.5, 130.3, 130.2, 130.1, 128.0, 127.9, 54.9, 48.5, 48.3, 47.8, 26.9, 22.0, 21.9 ppm. MS (FAB): m/z 879 $[M + H]^+$.

2,5,9,12-Tetraaza[13]metacyclophane (*m*-B232·4HBr): *m*-B232·4Ts (2.5 g, 2.8 mmol) and phenol (13 g, 144 mmol) were suspended in HBr/OHAc (33%, 140 mL). The mixture was stirred at 90 °C for 24 h. Then the heating was stopped and after several hours a solid appeared which was filtered and extensively washed with EtOH/CH_2Cl_2 (1:1); yield 1.3 g, 73%; m.p. 238–240 °C. ^{1}H NMR (D_2O, 300 MHz): δ = 7.79 (s, H), 7.70 (s, 3 H), 4.48 (s, 4 H), 3.51–3.43 (m, 4 H), 3.40–3.32 (m, 4 H), 3.15 (t, J = 8 Hz, 4 H), 2.00–1.89 (m, 2 H) ppm. ^{13}C NMR (D_2O, 75.43 MHz): δ = 135.2, 134.8, 134.2, 52.6, 45.8, 43.7, 42.4, 24.3 ppm. $C_{15}H_{30}N_4Br_4$ (586.07): calcd. C 30.7, H 5.2, N 9.6; found C 30.7, H 5.5, N, 9.4.

2,5,9,12-Tetraaza[13]paracyclophane (*p*-B232·4HBr·H_2O): This compound was obtained by the same procedure detailed for *m*-B232·4HBr; yield 1.5 g, 91%; m.p. 226–228 °C. ^{1}H NMR (D_2O, 300 MHz): δ = 7.69 (s, 4 H), 4.44 (s, 4 H), 3.32–3.37 (m, 4 H), 3.01–3.06 (m, 4 H), 2.96 (t, J = 8 Hz, 4 H), 1.49–1.55 (m, 2 H) ppm. ^{13}C NMR (D_2O, 75.43 MHz): δ = 132.1, 132.0, 50.6, 43.4, 41.3, 40.7, 20.5 ppm. $C_{15}H_{32}N_4OBr_4$ (604.09): calcd. C 29.8, H 5.3, N, 9.3; found C 29.6, H 5.3, N 9.2.

NMR Measurements: The ^{1}H and ^{13}C NMR spectra were recorded with a Bruker Advance AC-300 spectrometer operating at 299.95 MHz for ^{1}H and at 75.43 MHz for ^{13}C. For the ^{13}C NMR spectra, dioxane was used as a reference standard (δ = 67.4 ppm) and for the ^{1}H spectra, the solvent signal was used. Adjustments to the desired pH were made using drops of DCl or NaOD solutions. The pD was calculated from the measured pH values by using the correlation pH = pD – 0.4.[30]

Potentiometric Measurements: The potentiometric titrations were carried out at 298.1 ± 0.1 K using $NaClO_4$ (0.15 M) as the supporting electrolyte. The experimental procedure (burette, potentiometer, cell, stirrer, microcomputer, etc.) has been fully described elsewhere.[31] The acquisition of the emf data was performed with the PASAT computer program.[32] The reference electrode was a Ag/AgCl electrode in a saturated KCl solution. The glass electrode was calibrated as a hydrogen ion concentration probe by the titration of previously standardized amounts of HCl with CO_2-free NaOH solutions, and the equivalence point was determined by Gran's method,[33] which gives the standard potential, $E°'$, and the ionic product of water [pK_w = 13.73(1)].

The HYPERQUAD computer program was used to calculate the protonation and stability constants.[34] The 2.5–11.0 pH range was investigated and the concentration of the metal ions and of the ligands ranged from 1×10^{-3} to 5×10^{-3} mol dm^{-3} with M/L molar ratios varying from 2:1 to 1:2. The different titration curves for each system (at least two) were treated either as a single set or as separated curves without significant variations in the values of the stability constants. Finally, the data sets were merged together and treated simultaneously to give the final stability constants. The reported estimation of the errors corresponds in all cases to the standard deviation in the fit of the whole data set for a given system.

Kinetic Measurements: The decomposition kinetics of the Cu^{II} complexes with the *m*-B232, *p*-B232 and 232 ligands were studied at 298.1 K using an Applied Photophysics SX17MV stopped-flow spectrophotometer with a PDA.1 diode-array detector. Solutions of the metal complexes for the kinetic studies were prepared with a ligand concentration of 1.0×10^{-3} mol dm^{-3}, and the Cu^{II}/L ratio (1:1 or 2:1) and the pH of the starting solutions were selected from the species distribution curves so that the concentration of one of the complex species was at a maximum while that of the other ones was maintained at a minimum. For this reason, in general only those species which represent at least 80% of the total complex under some conditions were studied. The solutions of the starting complexes were mixed in the stopped-flow instrument with solutions containing an excess of acid under pseudo first-order conditions, which required in some cases dilution of the stock complex solution. The same procedure was used to study the kinetics of decomposition of the Cu(*o*-B232)$^{2+}$ complex, although this reaction occurs more slowly and was studied using a conventional Cary 50-Bio UV/Vis spectrophotometer. The kinetic experiments were carried out with the ionic strength adjusted to 0.15 mol dm^{-3} with $NaClO_4$ (*o*-B232 and *m*-B232) or NaCl (*p*-B232). For the case of the linear 232 ligand, the kinetic experiments were repeated using different supporting electrolytes ($NaClO_4$, NaCl and KNO_3) without significant differences between them.

The reaction kinetics was monitored either by recording the complete spectral changes with time (experiments with the conventional spectrophotometer and some stopped-flow experiments using the diode-array detector) or by measuring the absorbance changes at the wavelength of maximum absorption for each complex. In the first case the data were analyzed with the SPECFIT/32 program,[35] whereas for single wavelength measurements the standard software for the stopped-flow instrument was used. Consistent results were obtained using both fitting procedures. The reported estimation of the errors corresponds in all cases to the standard deviation in the fit of the data showing the changes of the observed rate constants with the proton concentration.

Supporting Information (see also the footnote on the first page of this article): Species distribution curves for the different protonated forms of the ligands and for their corresponding Cu^{II} complexes.

Acknowledgments

Financial support from the Spanish Dirección General de Investigación Científica y Técnica (DGICYT), research projects CTQ2006-15672-CO5-01 and CTQ2006-14909-CO2-01), Generalitat Valenciana (GV06/258) and Junta de Andalucía (FQM-137) is gratefully acknowledged. A. F. acknowledges a grant from the Programa de Doctorado Conjunto entre la Universidad de Cádiz y las Universidades Cubanas (Spain). J. M. Ll. thanks the Spanish Ministerio de Ciencia y Tecnología (MCYT) for a Ramón y Cajal contract.

[1] a) A. Bianchi, M. Micheloni, P. Paoletti, *Coord. Chem. Rev.* **1991**, *110*, 17–113; b) M. Izatt, K. Pawlak, J. S. Bradshaw, R. L. Bruening, *Chem. Rev.* **1995**, *95*, 2529–2586; c) E. García-España, P. Díaz, J. M. Llinares, *Coord. Chem. Rev.* **2006**, *250*, 2952–2986.

[2] a) J.-M. Lehn, *Angew. Chem. Int. Ed. Engl.* **1988**, *27*, 89–112; b) J.-M. Lehn, *Supramolecular Chemistry. Concepts and Perspective*, VCH, Weinheim, Germany, **1995**; c) F. P. Schmidtchen, *Top. Curr. Chem.* **1986**, *132*, 101–133; d) M. E. Huston, E. U. Akkaya, A. W. Czarnik, *J. Am. Chem. Soc.* **1989**, *111*, 8735–8737; e) B. Dietrich, *Pure Appl. Chem.* **1993**, *65*, 1457–1464; f) A. Bianchi, K. Bowman-James, E. Garcia-España *Supramolecular Chemistry of Anions*, Wiley-VCH, New York, **1997**; g) P. D. Beer, *Acc. Chem. Res.* **1998**, *31*, 71–80; h) P. D. Beer, P. A. Gale, *Angew. Chem. Int. Ed.* **2001**, *40*, 486–516; i) P. A. Gale, *Coord. Chem. Rev.* **2001**, *213*, 79–128; j) A. Bencini, A. Bianchi, E. García-España, M. Micheloni, J. A. Ramírez, *Coord. Chem. Rev.* **1999**, *188*, 97–156.

[3] G. Schwarzenbach, *Helv. Chim. Acta* **1952**, *35*, 2344–2359.

[4] R. Barbucci, L. Fabbrizzi, P. Paoletti, *Coord. Chem. Rev.* **1972**, *8*, 31–37.

[5] D. C. Weatherburn, E. J. Billo, J. P. Jones, D. W. Margerum, *Inorg. Chem.* **1970**, *9*, 1557–1559.

[6] P. Paoletti, L. Fabbrizzi, R. Barbucci, *Inorg. Chem.* **1973**, *12*, 1861–1864.

[7] T. G. Fawcett, S. M. Rudich, B. H. Toby, R. A. Lalancette, J. A. Potenza, H. J. Schugar, *Inorg. Chem.* **1980**, *19*, 940–945.

[8] G. Marongiu, E. C. Lingafelter, P. Paoletti, *Inorg. Chem.* **1969**, *8*, 2763–2767.

[9] J. M. Walshe, *Proc. R. Soc. Med.* **1977**, *70*, 1–3.

[10] a) H. Harders, E. Cohnen, *Proc. R. Soc. Med.* **1977**, *70*, 10–12; b) J. F. Pilichowski, M. Borel, G. Meyniel, *Eur. J. Med. Chem.* **1984**, *19*, 425–431; c) B. Sarkar, *Chem. Rev.* **1999**, *99*, 2535–2544.

[11] T. R. Borthwick, G. D. Benson, H. J. Schugar, *Proc. Soc. Exp. Biol. Med.* **1979**, *162*, 227–228.

[12] X. Sun, J. Kim, A. E. Martell, M. J. Welch, C. J. Anderson, *Nucl. Med. Biol.* **2004**, *31*, 1051–1059.

[13] a) F. Diederich, *Angew. Chem. Int. Ed. Engl.* **1988**, *27*, 362–386; b) F. Vogtle, P. R. Jones, *Cyclophane Chemistry: Synthesis Structures and Reactions*, John Wiley & Sons, New York, **1993**; c) R. Gleiter, H. Hopf (Eds.), *Modern Cyclophane Chemistry*, Wiley-VCH, Weinheim, **2004**.

[14] a) C. Bazzicalupi, A. Bencini, A. Bianchi, V. Fusi, E. Garcia-España, C. Giorgi, J. M. Llinares, J. A. Ramirez, B. Valtancoli, *Inorg. Chem.* **1999**, *38*, 620–621; b) E. Garcia-España, P. Gaviña, J. Latorre, C. Soriano, B. Verdejo, *J. Am. Chem. Soc.* **2004**, *126*, 5082–5083; c) B. Verdejo, J. Aguilar, A. Domenech, C. Miranda, P. Navarro, R. Jimenez Hermas, C. Soriano, E. Garcia-España, *Chem. Commun.* **2005**, 3086–3088.

[15] a) M. G. Basallote, A. Domenech, A. Ferrer, E. Garcia-España, J. M. Llinares, M. A. Manez, C. Soriano, B. Verdejo, *Inorg. Chim. Acta* **2006**, *359*, 2004–2014; b) J. Aguilar, M. G. Basallote, L. Gil, J. C. Hernandez, M. A. Máñez, E. Garcia-España, C. Soriano, B. Verdejo, *Dalton Trans.* **2004**, 94–103.

[16] a) M. Yoshida, M. Muneynki, T. Hisabori, *Nat. Rev. Mol. Cell Biol.* **2001**, *2*, 669; b) P. D. Boyer, *Nature* **1999**, *402*, 247–249; c) D. Stock, A. G. W. Leslie, J. E. Walker, *Science* **1999**, *286*, 1700–1705; d) K. Namba, F. Vonderviszt, *Q. Rev. Biophys.* **1997**, *30*, 1–65; e) M. Meister, S. R. Caplan, H. C. Berg, *Biophys. J.* **1989**, *55*, 905–914.

[17] A. Andrés, C. Bazzicalupi, A. Bianchi, E. García-España, S. V. Luis, J. F. Miravet, J. A. Ramírez, *J. Chem. Soc. Dalton Trans.* **1994**, 2995–3004.

[18] a) M. Chadim, P. Díaz, E. García-España, J. Hodacova, P. C. Junk, J. Latorre, J. M. Llinares, C. Soriano, J. Zavada, *New J. Chem.* **2003**, *27*, 1132–1139; b) M. Chadim, M. Budesinsky, J. Hodacova, J. Zavada, *Collect. Czech. Chem. Commun.* **2000**, *65*, 99–105.

[19] C. Nave, M. Truter, *J. Chem. Soc. Dalton Trans.* **1974**, 2351–2354.

[20] M. Studer, A. Riesen, T. A. Kaden, *Helv. Chim. Acta* **1989**, *72*, 1253–1258.

[21] J. E. Sarnesky, H. L. Surprenant, F. K. Molen, C. N. Reiley, *Anal. Chem.* **1975**, *47*, 2116–2124.

[22] a) R. Menif, A. E. Martell, P. J. Squattrito, A. E. Clearfield, *Inorg. Chem.* **1990**, *29*, 4723–4729; b) M. G. Basallote, J. Durán, M. J. Fernández-Trujillo, M. A. Máñez, B. Szpoganicz, *J. Chem. Soc. Dalton Trans.* **1999**, 1093–1100; c) M. Kodama, *Bull. Chem. Soc. Jpn.* **1997**, *70*, 1361–1367; d) M. Kodama, E. Kimura, *J. Chem. Soc. Dalton Trans.* **1978**, 1081–1085.

[23] M. J. Fernández-Trujillo, B. Szpoganicz, M. A. Máñez, L. T. Kist, M. G. Basallote, *Polyhedron* **1996**, *15*, 3511–3517.
[24] L. H. Chen, C. S. Chung, *Inorg. Chem.* **1989**, *28*, 1402–1405.
[25] a) R. Read, D. W. Margerum, *Inorg. Chem.* **1981**, *20*, 3143–3149; b) S. Siddiqui, R. E. Shepherd, *Inorg. Chem.* **1983**, *22*, 3726-.3733.
[26] a) R. W. Hay, R. Bembi, W. T. Moodie, P. R. Norrhan, *J. Chem. Soc. Dalton Trans.* **1982**, 2131–2136; b) L. Fabbrizzi, T. A. Kaden, A. Perotti, B. Seghi, L. Siegfried, *Inorg. Chem.* **1986**, *25*, 321–327; c) R. W. Hay, M. Tofazzal, H. Tarafder, M. M. Hassan, *Polyhedron* **1996**, *15*, 725; d) W. J. Lan, C. S. Chung, *J. Chem. Soc. Dalton Trans.* **1994**, 191–194; e) G. De Santis, L. Fabbrizzi, A. Perotti, N. Sardone, A. Taglietti, *Inorg. Chem.* **1997**, *36*, 1998–2003; f) M. G. Basallote, J. Durán, M. J. Fernández-Trujillo, M. A. Máñez, *J. Chem. Soc. Dalton Trans.* **2002**, 2074–2079.
[27] B. Verdejo, A. Ferrer, S. Blasco, C. E. Castillo, J. González, J. Latorre, M. A. Máñez, M. G. Basallote, C. Soriano, E. García-España, *Inorg. Chem.* **2007**, *46*, 5707–5719.
[28] a) J. W. Chen, D. W. Wu, C. S. Chung, *Inorg. Chem.* **1986**, *25*, 1940–1943; b) L. H. Chen, C. S. Chung, *Inorg. Chem.* **1988**, *27*, 1880–1883; c) B. F. Liang, C. S. Chung, *Inorg. Chem.* **1983**, *22*, 1017–1021.
[29] M. G. Basallote, J. Durán, M. J. Fernández-Trujillo, M. A. Máñez, *J. Chem. Soc. Dalton Trans.* **1999**, 3817–3823.
[30] A. K. Covington, M. Paabo, R. A. Robinson, R. G. Bates, *Anal. Chem.* **1968**, *40*, 700–706.
[31] E. García-España, M. J. Ballester, F. Lloret, J. M. Moratal, J. Faus, A. Bianchi, *J. Chem. Soc. Dalton Trans.* **1988**, 101–104.
[32] M. Fontanelli, M. Micheloni, *Proceedings of the 1st Spanish-Italian Congress on Thermodynamics of Metal Complexes*, Peñíscola, Castellón, **1990**. Program for the automatic control of a microburette and the acquisition of the electromotive force reading.
[33] a) G. Gran, *Analyst (London)* **1952**, *77*, 661–671; b) F. J. Rossotti, H. Rossotti, *J. Chem. Educ.* **1965**, *42*, 375–378.
[34] P. Gans, A. Sabatini, A. Vacca, *Talanta* **1996**, *43*, 1739–1753.
[35] R. A. Binstead, B. Jung, A. D. Zuberbühler, *SPECFIT-32*, Spectrum Software Associates, Chapel Hill, **2000**.

Received: October 13, 2007
Published Online: January 29, 2008

